Earth and Planetary Science Letters 402 (2014) 209–220

Contents lists available at ScienceDirect

Earth and Planetary Science Letters

www.elsevier.com/locate/epsl

Mantle flow and lithosphere–asthenosphere coupling beneath the southwestern edge of the North American craton: Constraints from shear-wave splitting measurements

Hesham A. Refayee, Bin B. Yang, Kelly H. Liu, Stephen S. Gao *

Department of Geological Sciences and Engineering, Missouri University of Science and Technology, Rolla, MO 65409, USA

ARTICLE INFO

Article history:
Accepted 25 January 2013
Available online 22 February 2013
Editor: P. Shearer

Keywords:
seismic anisotropy
shear–wave splitting
mantle flow

ABSTRACT

High-quality broadband seismic data recorded by the USArray and other stations in the southwestern United States provide a unique opportunity to test different models of anisotropy-forming mechanisms in the vicinity of a cratonic margin. Systematic spatial variations of anisotropic characteristics are revealed by 3027 pairs of splitting parameters measured at 547 broadband seismic stations. The western and southern edges of the North American craton show edge-parallel fast directions with larger-than-normal splitting times, and the continental interior is characterized by smaller splitting times and spatially consistent fast directions that are mostly parallel to the absolute plate motion direction of North America. At the majority of the stations, no significant systematic azimuthal variations of the splitting parameters are observed, suggesting that a single layer of anisotropy with a horizontal axis of symmetry can adequately explain most of the observations. The spatial coherency of the splitting parameters indicates that the observed anisotropy is likely caused by shearing between the partially coupled lithosphere and asthenosphere. Based on previous results of seismic tomography and geodynamic modeling, we propose a model involving deflecting of asthenospheric flow by the cratonic root as the cause of the observed edge-parallel fast directions and large splitting times along the western and southern edges of the North American craton.

1. Introduction

Shear-wave splitting (SWS) analysis is one of the most commonly used techniques in structural seismology. The two resulting splitting parameters, the polarization direction of the fast wave (ϕ or fast direction) and the arrival time difference between the fast and slow waves (δt or splitting time), are respectively indicators of the orientation and strength of seismic anisotropy accumulated along the ray path. The *P*-to-*S* converted waves at the core–mantle boundary (*XKS*, which includes *SKS*, *SKKS*, and *PKS*) are ideal for SWS analysis, due to the fact that the initial polarization direction is along the radial direction and thus any energy in the *XKS* window on the transverse component is an indicator of azimuthal anisotropy (Silver and Chan, 1991).

While the splitting parameters can usually be reliably determined, at the present time, the interpretation of the resulting splitting parameters is still an unsettled and debated issue. Numerous laboratory and modeling studies indicate that lattice preferred orientation (LPO) of the crystallographic axes of olivine is a possible cause of mantle anisotropy (Zhang and Karato, 1995). Except for areas with extreme anomalies in temperature, pressure, and water content, these studies suggest that the fast direction of A-type olivine fabric is subparallel to the LPO of the *a*-axis of olivine (Karato et al., 2008). The implication of SWS observations is complicated by the fact that there are more than one mantle processes that can lead to the LPO, among which the most important ones are simple shear originated from flow gradient in the asthenosphere, which leads to a fast direction that is parallel to the flow direction, and lithospheric compression which results in anisotropy with a fast direction parallel to the strike of the mountain belts (Silver, 1996; Savage, 1999; Fouch and Rondenay, 2006; Long and Silver, 2009). Adding to this ambiguity in the interpretation of SWS measurements is the hypothesis that magmatic dikes in the lithosphere, when aligned preferably along a certain direction, can also lead to observable seismic anisotropy with a dike-parallel fast direction (Gao et al., 1997; Walker et al., 2004; Kendall et al., 2005). Beside A-type fabric of olivine and aligned magmatic dikes, other anisotropy-forming mechanisms in the upper mantle have been proposed (e.g., Holtzman et al., 2003; Karato et al., 2008), but the thermal, pressure, and water content anomalies needed for them to dominate are unlikely to exist in the study area.

* Corresponding author. Tel.: +1 573 341 6676.
E-mail addresses: har5gd@mst.edu (H.A. Refayee), bych9@mst.edu (B.B. Yang), liukh@mst.edu (K.H. Liu), sgao@mst.edu (S.S. Gao).

0012-821X/$ - see front matter © 2013 Elsevier B.V. All rights reserved.
http://dx.doi.org/10.1016/j.epsl.2013.01.031

Whether seismic anisotropy observed in a given area is of lithospheric or asthenospheric origin (and/or whether it is affected by compression or diking within the lithosphere) is the key information needed for useful interpretation of SWS measurements. Unfortunately, due to the steep angle of incidence of the *XKS* waves, the vertical resolution of the SWS technique is low. To some extent, surface wave dispersion studies can resolve the depth distribution of seismic anisotropy (Montagner, 1998; Yuan and Romanowicz, 2010), but the resolution in both vertical and horizontal directions is intrinsically limited relative to body-wave studies. Recently, Liu and Gao (2011) proposed a procedure to estimate the depth of the source of anisotropy using the spatial variability of splitting parameters. This technique requires the availability of high-quality SWS measurements obtained at densely spaced seismic stations. As discussed below, the study area (Fig. 1) is well sampled by stations in the ongoing USArray project, which has a nominal station spacing of 70 km and has recorded an outstanding data set for characterizing the 3-D distribution of seismic anisotropy in the mantle beneath the study area.

Another issue that can be constrained using SWS analysis is the degree of coupling between the lithosphere and the underlying asthenosphere. Global-scale anisotropy studies using surface waves suggest that the asthenosphere beneath most slow-moving continents is nearly isotropic, implying decoupling between the lithosphere and asthenosphere except for Australia which is the fastest moving continent (Debayle et al., 2005). Decoupling is also advocated by others to explain westward net drift of the lithosphere relative to the mesosphere (Doglioni et al., 2011), and to explain geoid anomalies across transform faults that separate ocean floors of different age (Craig and McKenzie, 1986). Most of these studies suggest the existence of an ultra-thin, low viscosity layer immediately beneath the lithosphere. This layer prevents transfer of shear stress between the lithosphere and the asthenosphere, leading to decoupling of the two. However, some geodynamic modeling and seismic anisotropy studies suggest a high-degree coupling between the two layers (Becker and O'Connell, 2001; Marone and Romanowicz, 2007; Bird et al., 2008). A combination of the broadband seismic data set and the tectonic setting of the study area provides an excellent opportunity to address this problem.

The bulk of the study area consists of the southeastern part of the western US orogenic zone and the southern Great Plains, which are approximately separated by the eastern edge of the Rio Grande Rift in the study area (Fig. 1). Two suture zones divide the Proterozoic basement into three provinces, which become progressively younger toward the southeast (Thomas, 2006; Whitmeyer and Karlstrom, 2007). Major tectonic features include the Rio Grande Rift, the Southern Oklahoma Aulacogen, and the continental-oceanic transitional crust formed as a result of extension during the formation of the Gulf of Mexico (Mickus et al., 2009). Seismic body-wave and surface wave tomography

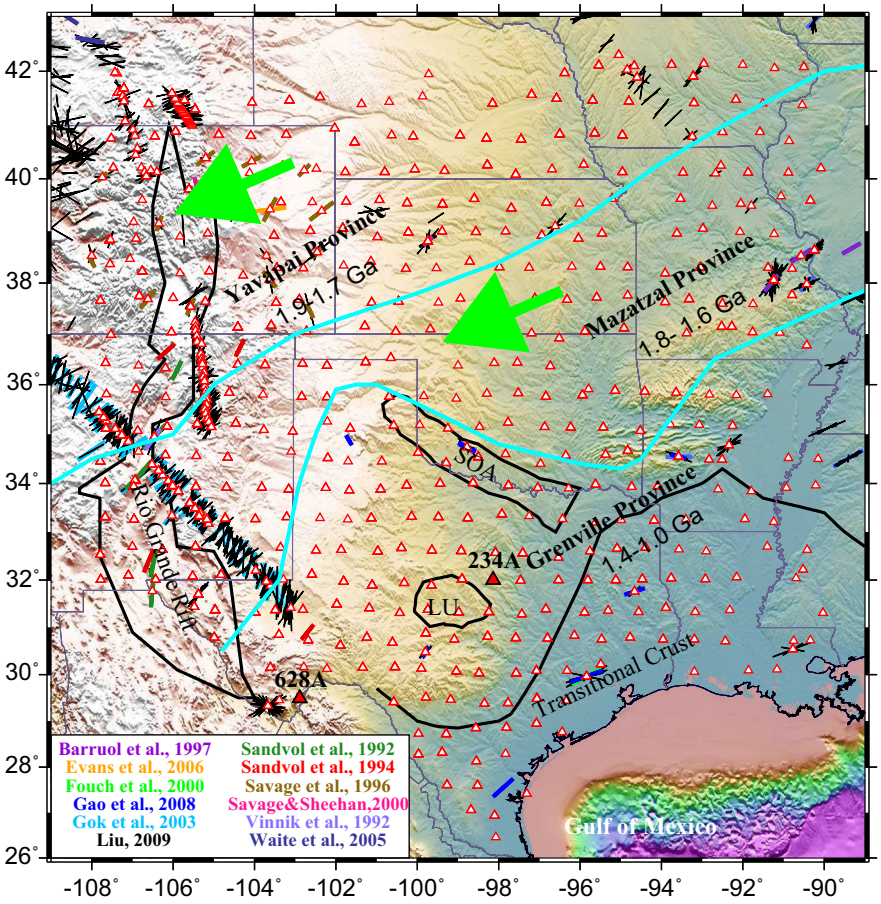

Fig. 1. Topographic relief map of the study area showing seismic stations used in the study (triangles) and major tectonic provinces. The solid blue lines separate Precambrian basement terranes (Thomas, 2006; Holm et al., 2007), and the green arrows indicate the direction of the absolute plate motion (APM) of the North American Plate (Gripp and Gordon, 2002). Example data from the two named stations (234A and 628A) are shown in Fig. 3. SOA: Southern Oklahoma Aulacogen; LU: Llano Uplift. Also shown are previous shear-wave splitting measurements in the study area (Barruol et al., 1997; Evans et al., 2006; Fouch et al., 2000; Gao et al., 2008; Gok et al., 2003; Liu, 2009; Sandvol et al., 1992; Sandvol and Ni, 1994; Savage et al., 1996; Savage and Sheehan, 2000; Vinnik et al., 1992; Waite et al., 2005). For a given study, the same color is used for the citation in the legend and the bars in the map.

studies (van der Lee and Nolet, 1997; Yuan and Romanowicz, 2010; Burdick et al., 2012) suggest that the lithosphere beneath the Great Plains has a thickness of about 200–250 km, and thins to about 125 km beneath the western US orogenic zone and beneath the area with transitional crust (Wilson et al., 2005; van der Lee and Frederiksen, 2005; Yuan and Romanowicz, 2010).

This area is an ideal locale for addressing the three-dimensional (3-D) distribution of seismic anisotropy and for investigating coupling between the lithosphere and asthenosphere, for several reasons: (1) It is well-sampled by the EarthScope Transportable Array (TA), the densely spaced stations in which allow reliable determination of the depth of the source of anisotropy using spatial variation factors. (2) There is a diverse set of tectonic features with anticipated spatially varying lithospheric thickness and mantle fabric directions and strength that can be quantified by SWS analysis. (3) The upper mantle structure beneath the area has been investigated by numerous studies and thus provides a solid foundation for meaningful interpretations of the SWS results.

2. Tectonic setting and previous seismic anisotropy studies

The southwestern part of the contiguous United States has experienced a significant amount of deformation and magmatism from the Precambrian to the Cenozoic Era (Whitmeyer and Karlstrom, 2007; Karlstrom and Bowring, 1988). These orogenic events include the late Proterozoic Yavapai orogeny (1.71–1.68 Ga), the Mazatzal orogeny (1.7–1.65 Ga), and the Grenville orogeny (1.3–0.9 Ga) (Whitmeyer and Karlstrom, 2007). During the Proterozoic, the basement of the continental crust was rapidly generated by accretion of several major volcanic arcs (Hoffman, 1988, 1989; Condie, 1982; Karlstrom and Bowring, 1988). The widespread extension, which took place during the Cenozoic created magmatic episodes in the Tertiary (Coward et al., 1987; Baldridge et al., 1991; Balch et al., 1997; McMillan et al., 2000), uplifted the Colorado Plateau (Liu and Gurnis, 2010) and formed the Rio Grande Rift (Morgan et al., 1986; Mosher, 1998; Lawton and McMillan, 1999).

In the study area, a number of SWS and other seismic anisotropy studies were conducted during the pre-USArray era (Fig. 1). A study conducted by Savage and Sheehan (2000) measured *SKS* splitting using data from the Colorado Plateau-Great Basin portable array stations. They observed NE–SW fast direction beneath both the Rio Grande Rift and the Rocky Mountains with a splitting time of 1.0 s. Sandvol et al. (1992) reported N–S fast directions in the Rio Grande Rift at five portable stations. Gok et al. (2003) and Wang et al. (2008) found that the fast directions are N–S to NE–SW within the southeastern section of the rift. Splitting times of 1.4 s were found.

Gao et al. (2008) conducted shear wave splitting measurements at permanent broadband stations in the south-central United States. They attributed the observed anisotropy to magmatic dikes in the lithosphere and/or asthenospheric flow. In our study area, using joint inversion of surface waveform and a limited number of *SKS* splitting measurements, Yuan and Romanowicz (2010) proposed two distinct layers. The upper layer, which resides in the lithosphere, has a N–S fast direction, and the lower layer, which is in the upper asthenosphere, is dominated by a NE–SW fast direction.

3. Data and methods

The study area ranges from 109°W–90°W and 26°N–42°N. Broadband seismic data from all the USArray and permanent stations in the study area were requested from the IRIS (Incorporated Research Institutions for Seismology) DMC (Data Management Center). For stations in the western US orogenic zone (approximately west of 105°W) where rapid spatial variation of anisotropy is expected, we also requested data from portable seismic experiments. Data from most of the stations ended around early 2012. The cutoff magnitude for events with a focal depth $\leq$ 100 km is 5.6, and that for deeper events is 5.5 to take the advantage of the sharper waveforms normally associated with deep events. The epicentral distance range used is 120–180° for PKS, and 84–180° for *SKKS* and *SKS* (Gao and Liu, 2009).

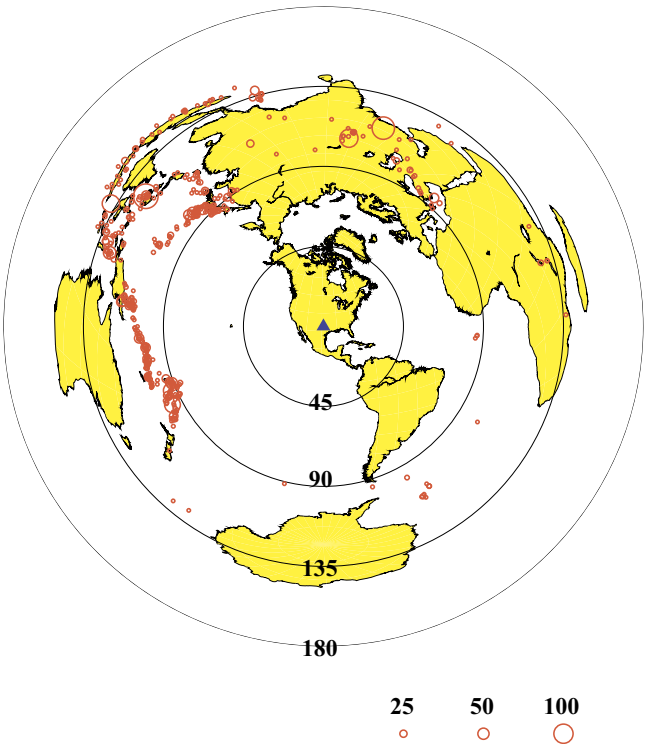

Fig. 2. Azimuthal equidistant projection map showing the distribution of 475 earthquakes used in the study. Size of the red circles is proportional to the number of resulting well-defined splitting measurements. The black circles and corresponding labels show the distance in degree to the center of the study area. (For interpretation of the references to color in this figure legend, the reader is referred to the web version of this article.)

Following the procedure of Liu (2009), which was based on the minimization of transverse energy approach (Silver and Chan, 1991), we resampled the seismograms into a uniform sampling rate of 20 sps, and band-pass filtered them in the frequency band of 0.04–0.5 Hz which contains most of the *XKS* energy. All the measurements were visually inspected and if necessary, data processing parameters such as the beginning and ending time of the *XKS* window, band-pass filtering parameters, and automatically determined ranking (Liu et al., 2008) were adjusted manually. Figs. 1 and 2 show the distribution of the stations and events, respectively, and Fig. 3 shows examples of *XKS* phases and various figures associated with the data processing procedure.

4. Spatial variations of resulting splitting parameters

A total of 3027 pairs of well-defined (Quality A and B, see Liu et al., 2008 for details about ranking criteria) splitting parameters were obtained from 475 events at 547 stations. Among them 2238 are *SKS*, 406 are *SKKS*, and 383 are *PKS* measurements. The mean splitting time over all the measurements is 1.01 ± 0.34 s

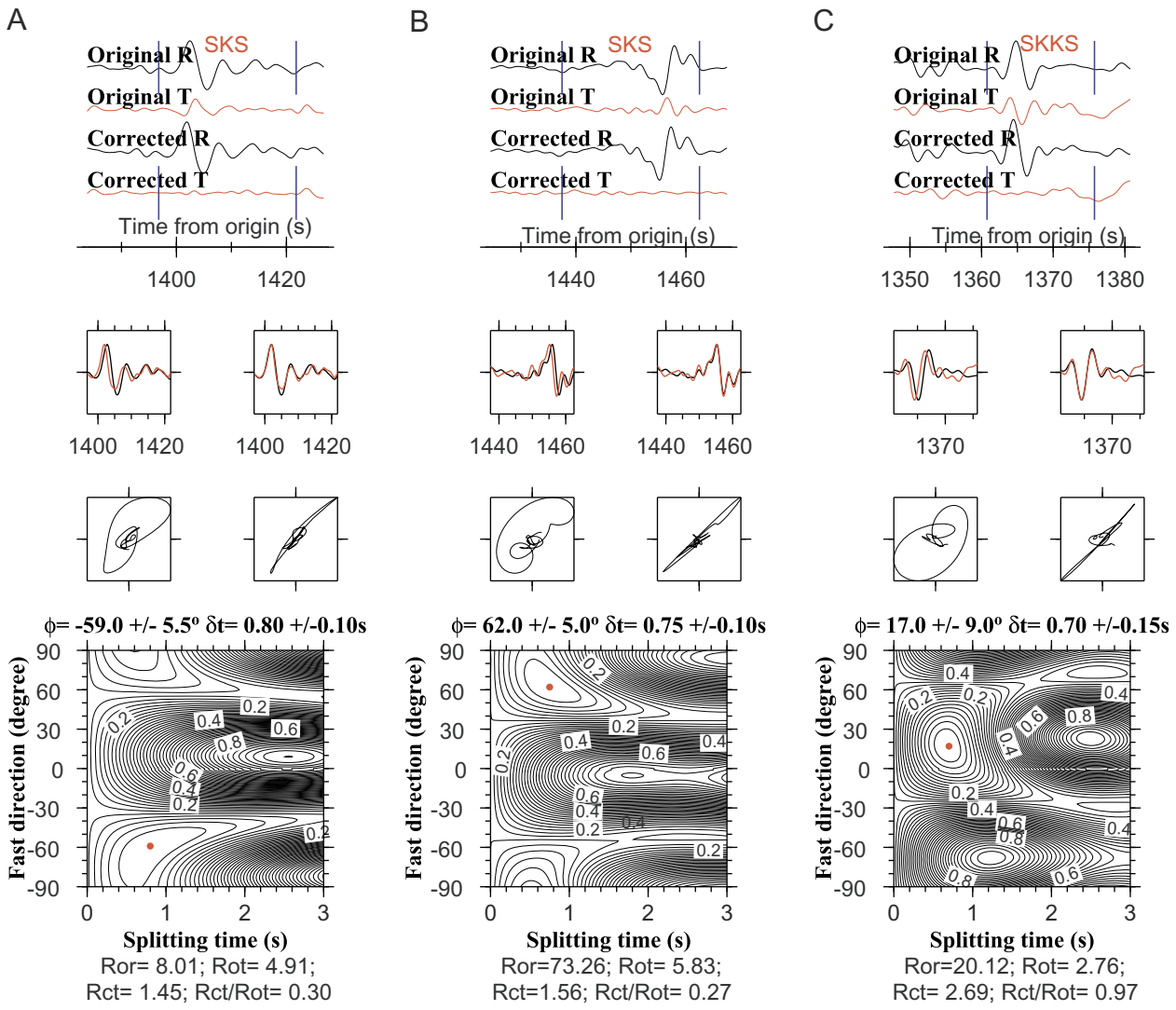

Fig. 3. Original and corrected XKS seismograms (top panels), particle motion patterns (middle), and the contour maps of transverse component energy (bottom) from stations 628A_TA (A) and 234A_TA (B and C). The back-azimuth (and origin time) for the three events is 237° (2009-116-00-06), 8° (2011-200-19:35), and 241° (2009-230-21-20), respectively. The red dot on the contour map indicates the optimal splitting parameters. (For interpretation of the references to color in this figure legend, the reader is referred to the web version of this article.)

which is identical to the global average of 1.0 s (Silver, 1996). For a commonly assumed degree of anisotropy of 4% (Mainprice et al., 2000), the thickness of the anisotropic layer is about 110 ± 30 km. Note that the uncertainties presented in this paper are one standard deviation. The resulting SWS parameters (Figs. 4 and 5) show systematic spatial variations and close correspondence with the absolute plate motion (APM) (Gripp and Gordon, 2002) and geological provinces. Fast directions observed in the western US orogenic zone and the western margin of the Great Plains are dominantly N–S, while the rest of the study area shows mostly NE–SW fast directions (Fig. 4).

We divide the study area into four regions based on the characteristics of the SWS measurements and also on Proterozoic basement provinces. Area A, which contains 1388 pairs of measurements from 253 stations, is the east-most portion of the western US orogenic zone and the western margin of the Great Plains. The mean fast direction in this area is $28 \pm 23°$, and the mean splitting time is 1.05 ± 0.35 s. Area B is the southern part of the Yavapai province and contains 421 pairs of SWS measurements from 62 stations. The mean fast direction is $64 \pm 22°$, and the mean splitting time is 0.89 ± 0.28 s. Area C is the Mazatzal province and contains 367 pairs of measurements from 87 stations, and the mean splitting parameters are $57 \pm 25°$ and 0.86 ± 0.29 s. Area D is the Grenville province. This area has 851 pairs of measurement from 145 stations. The mean splitting time of 1.15 ± 0.36 s is the largest among the four areas, and the mean fast direction is $63 \pm 21°$. The southern part of Area D is on the continental-oceanic transitional crust. The 281 measurements on the transitional crust result in a mean splitting time of 1.23 ± 0.32 s and a mean fast direction of $67 \pm 15°$.

4.1. Fast directions

To illustrate the spatial variation of the fast directions and to explore their relationship with the APM direction, we calculate the APM direction for each of the 3027 ray-piercing points (at the depth of 200 km) based on the fixed hot-spot model of Gripp and Gordon (2002), and obtain the absolute difference between the two directions in the range of 0–90°. The resulting differences are then spatially averaged in 1° by 1° overlapping blocks with a moving step of 0.1°.

The resulting image (Fig. 4) indicates that beneath the western US orogenic zone and the western margin of the Great Plains, the

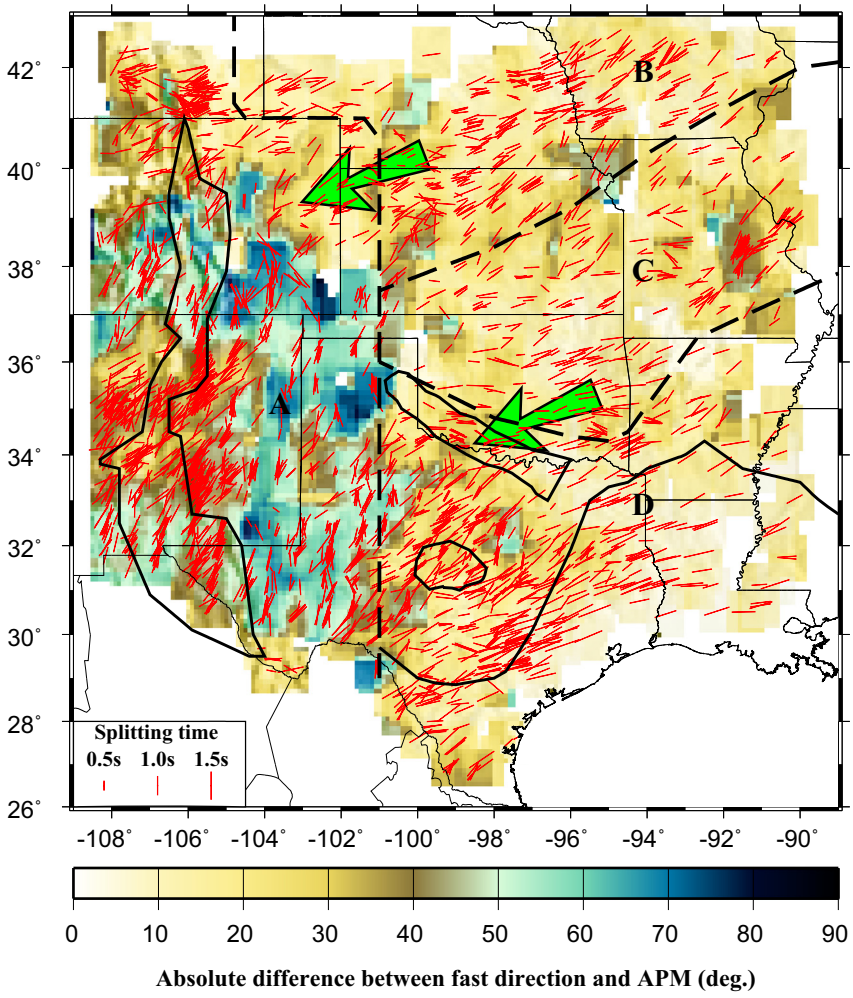

Fig. 4. Well-defined shear-wave splitting measurements. The orientation of the red bars represents the fast polarization direction, and the length is proportional to the splitting time. The background image shows absolute difference between the observed fast directions and the APM (arrows). The dashed lines separate areas with distinct basement ages, tectonic history and/or characteristics of the observed splitting parameters.

fast directions are about 50–70° away from APM. In contrast, the fast directions and APM are largely consistent beneath the central Great Plains and the transitional crust, with a few exceptions. The first is an area centered at (99°W, 31°N) in central Texas, tectonically known as the Llano Uplift (Mosher, 1998). The fast directions in this area are more northerly and vary spatially. As discussed in the next section, this apparent deviation of the fast direction from the APM direction is caused by azimuthal variations of the splitting parameters as a result of double layer anisotropy. The second area with large deviations is a band along the boundary between the Yavapai and Mazatzal provinces (Fig. 4). This band departs from the boundary at about 95°W and extends eastward. The large deviations are caused by the fact that the fast directions are spatially less consistent relative to the other areas of the Great Plains. The third area, although not as profound as the two above, is located at the southern-most tip of Texas. Here, the fast axes are oriented more northerly than the rest of the stations on the transitional crust. This observation, when combined with the relatively small splitting times in this area (Fig. 5) and the shape of the North American cratonic root, has important significance about the flow pattern around the cratonic keel, as discussed below. Finally, the six measurements at the southern-most tip of the Rio Grande Rift are mostly E–W oriented (Fig. 4), suggesting a possible termination of the N–S domain to the north. Fig. 3A shows an example of these measurements.

4.2. Splitting times

The spatial distribution of splitting times shown in Fig. 5 was produced by averaging the individual splitting times at piercing points of 200 km deep in overlapping 1° by 1° blocks with a moving step of 0.1°. The largest splitting times of ≥ 1.4 s are found in the vicinity of the Rio Grande Rift and in the area covered by transitional crust. A closer examination of the spatial distribution of the splitting times (Fig. 5) suggests that the area with the largest δt values has a coastline that is parallel to the APM. Near the western extreme of the area covered by transitional crust, where the coastline of the Gulf of Mexico becomes N–S, the δt values reduce to about 1.0 s.

The continental interior is characterized by small splitting times of 0.7–0.9 s. The smallest values are located along the suture zone separating the Yavapai and Mazatzal provinces. Interestingly, this is approximately the same area with the largest deviations between the fast directions and APM in the continental interior (Fig. 4).

5. Discussion

5.1. Stratification of seismic anisotropy

Azimuthal variations of splitting parameters with a $\pi/2$ periodicity is a diagnostic of double-layer anisotropy with a horizontal axis

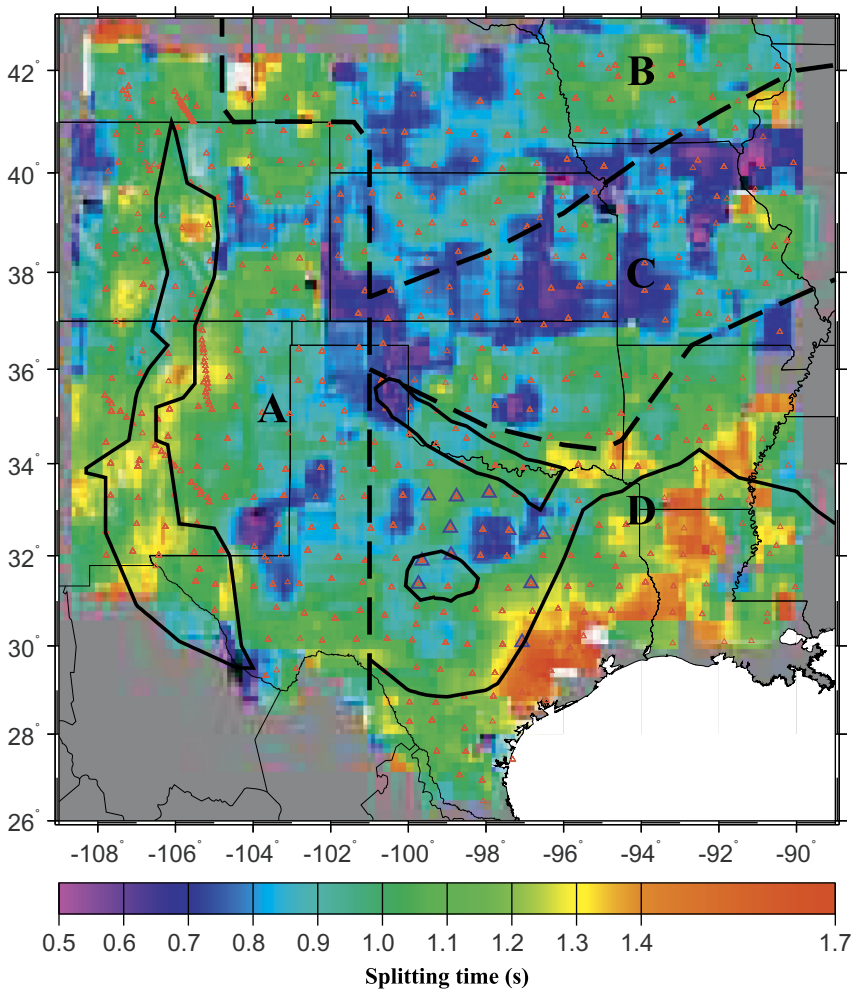

Fig. 5. Spatial distribution of splitting times. Red triangles represent seismic stations used in the study. Dashed lines represent boundaries between the four areas. Stations represented by blue triangles show systematic azimuthal variation of splitting parameters shown in Fig. 6. (For interpretation of the references to color in this figure legend, the reader is referred to the web version of this article.)

of symmetry (Silver and Savage, 1994). We visually examined splitting parameters for all the 547 stations and found that 13 of them (see Fig. 5 for their locations) show the most clear systematic azimuthal variations. They are located in the vicinity of the Llano Uplift, which is a Precambrian basement uplift in north-central Texas (Mosher, 1998). Fig. 3B and C show examples of *XKS* data recorded by the same station. Significantly different shear-wave splitting parameters are obtained from the two events, which have different back-azimuths.

We next attempt to grid-search for the two pairs of splitting parameters that fit the observed data at the 13 stations the best, using the approach of Silver and Savage (1994). Because there are normally more than one group of splitting parameters that can fit the data equally well (Gao and Liu, 2009), we use results from the surface-wave inversion of Yuan and Romanowicz (2010) as *a priori* constraints. In our study area, Yuan and Romanowicz (2010) reported a double-layer anisotropic structure. The top layer, which resides in the lithosphere and is about 150–250 km thick, has an approximately N–S fast direction and a relatively weak anisotropy (about 1.5%). This layer can result in a splitting time of about 0.6–0.8 s for a nearly vertically propagating *XKS* wave. The bottom layer has an APM-parallel fast direction (about 70°) and a stronger anisotropy of about 2.5% across most of our study area. Assuming a thickness of 200 km, the corresponding splitting time is about 1 s. Fig. 6 shows the theoretical splitting parameter curves calculated using surface wave inversion results (0° and 0.75 s for the top layer, and 70° and 1.0 s for the lower layer). Although the misfits are obvious, the general trends of the computed lines follow those of the observed data closely, especially for the fast directions.

To obtain a better fit, we search the optimal set of parameters in the vicinity of the surface-wave derived fast directions and free-varying splitting times, that is (40–90°, 0.0–2.0 s) for the lower layer, and (−25° to 25°, 0.0–2.0 s) for the top layer. The resulting best-fitting parameters are (60°, 1.3 s) for the lower layer, and (−19°, 0.4 s) for the top layer. The green lines in Fig. 6 are computed using the best-fitting parameters.

On the Llano Uplift and surrounding areas, the azimuthal variations of our SWS parameters and results from the grid-search above are in agreement with the surface-wave inversion results of Yuan and Romanowicz (2010). However, Yuan and Romanowicz (2010) also observed the existence of lithospheric anisotropy with a nearly N–S fast direction in the rest of our study area, and the majority of our SWS measurements do not show significant systematic azimuthal variations. One of the possible causes for the discrepancy could be the large difference in the frequency bands of the seismic waves used by the two types of studies. Surface waves have much longer period and thus are capable of detecting long-wavelength features. Small-scale (relative to the wavelength) heterogeneities in anisotropic properties in the lithosphere are smoothed out. On the other hand, *XKS* waves have shorter wavelength and consequently such

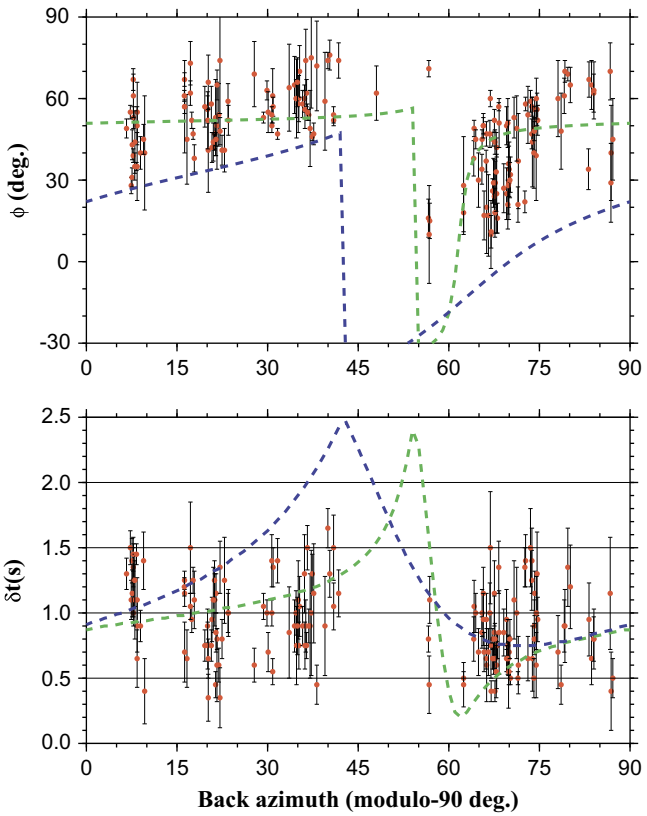

Fig. 6. Azimuthal variations of fast directions (top plot) and splitting times (bottom plot) for the 13 stations shown in Fig. 5. The green lines were computed using the optimal splitting parameters from grid-searching under a two-layer model, and the blue lines were computed using approximate splitting parameters estimated based on inversion of surface waveforms (Yuan and Romanowicz, 2010), by assuming an XKS frequency of 0.2 Hz. (For interpretation of the references to color in this figure legend, the reader is referred to the web version of this article.)

heterogeneities can have a significant impact on the results. If the heterogeneities are strong enough in the form of multiple layers and/or dipping axis of symmetry, the effect of anisotropy as observed by *XKS* waves can be canceled out. The fact that stations in the vicinity of the Llano Uplift show clear two-layer anisotropy suggests a relatively homogeneous anisotropic structure in the lithosphere beneath this area.

5.2. Estimating the depth of anisotropy beneath the study area

Previous studies revealed that the fast directions are mostly parallel to the APM direction or align with the strike of the geological features (Silver and Chan, 1991; Silver, 1996). Thus, the observed seismic anisotropy using SWS is either of lithospheric or asthenospheric or a combination of the two (Long and Silver, 2009; Savage, 1999). If the fast direction is in alignment with the absolute plate motion, the splitting parameters will primarily reflect an asthenosphere source (Conrad et al., 2007). Plate motion will enhance the mineral to orient, preferably, into the direction of the infinite strain axes. Therefore, the fast directions will be parallel to either the absolute plate motion shear or the mantle flow direction (Karato et al., 2008; Huang et al., 2011). Conversely, if the anisotropy has a lithospheric origin, the observed fast directions are expected to be parallel to the surface geological features (Nicolas and Christensen, 1987; Nicolas, 1993; Savage, 1999; Silver, 1996). Mountain belts, major fault zones, and continental and oceanic rifts including continental margins are likely places in which anisotropy will exist in the lithosphere (Silver, 1996). The key information to distinguish between lithospheric and asthenospheric origins of observed anisotropy is a reliable determination of the depth of the source of anisotropy.

Determination of the anisotropic depth is still a topic of argument in shear wave splitting studies. The source of anisotropy can in principle occur anywhere from the core–mantle boundary to the recording station at the surface (Barruol and Hoffmann, 1999; Gao et al., 2010). In this study, we use a spatial variation factor approach (Gao et al., 2010; Liu and Gao, 2011) to estimate the depth of anisotropy. A detailed description of this approach (and an accompanying freely accessible FORTRAN program) can be found in Gao and Liu (2012), and is briefly summarized below.

The procedure is built upon the principle that for a given *XKS* ray path traveling through an interface, the distance between the recording station and the surface projection of the ray-piercing point at the interface increases for deeper interface. When multiple events from various azimuths are recorded by closely spaced stations, the splitting parameters observed at the surface reach the highest spatial coherency if the interface is placed at the true depth. In practice, the optimal depth is searched by assuming a series of depths from 0 to 400 km at an interval of 5 km. The spatial variation factor as defined in Liu and Gao (2011), F_v, is computed for each of the assumed depths. The optimal depth corresponds to the minimum F_v.

The resulting F_v curves for the four areas are shown in Fig. 7. Beneath the western US orogenic zone and the area covered by transitional crust north of the Gulf of Mexico, the depth-estimate procedure found that the main contribution to the observed anisotropy is from a depth of about 150 km, and beneath the Great Plains, it is in the range of 200–250 km. These values remarkably agree with the thickness of the lithosphere beneath the respective areas estimated using various seismic techniques (van der Lee and Nolet, 1997; Wilson et al., 2005; Yuan and Romanowicz, 2010; Burdick et al., 2012). Such agreements suggest that the observed anisotropy mostly come from the top of the asthenosphere and/or the base of the lithosphere.

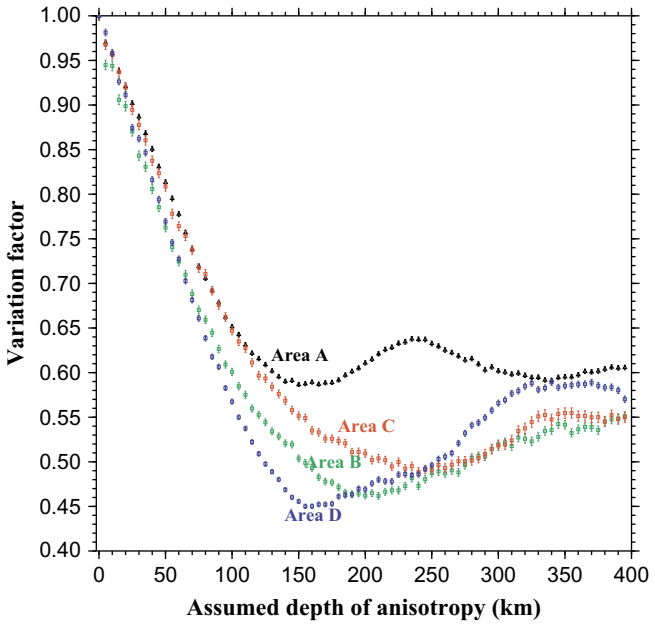

Fig. 7. Spatial variation factors as a function of assumed depth of the source of anisotropy for each of the four areas, estimated using the approach of Gao and Liu (2012).

5.3. Locating the edge of the North American craton

As discussed below, the observed anisotropy patterns are largely controlled by the edge of the North American craton. To obtain a first-order estimate of the shape of the cratonic edge, we obtained and processed data from all the USArray TA stations in the study area, from teleseismic earthquakes (in the epicentral distance range of 30–180°). The cutoff magnitude used for data requests is a function of focal depth and epicentral distance, as described in Liu and Gao (2010). The vertical components are then filtered in the frequency band of 0.04–1.0 Hz. An automatic trace-selection procedure is applied to the filtered seismograms to select those with a strong first arrival. The procedure utilizes the ratio between the absolute maximum value in the signal window and the mean absolute value of a noise window before the first arrival. Those selected for further processing have a ratio of 4.0 or greater. For a given event, the waveform cross-correlation approach (Vandecar and Crossen, 1990) was used to pick the relative travel-time residual relative to the IASPEI91 standard earth model (Kennett and Engdahl, 1991) at each station, and the residuals for all the events at each station are averaged to obtain a mean residual for each of the stations. A larger residual indicates slower average velocity along the ray path, and vice versa. Because the lithosphere has higher velocities than the asthenosphere, larger residuals usually suggest thinner lithosphere.

The results shown in Fig. 8 are obtained by smoothing the station averages in 1° by 1° moving windows with a moving step of 0.1°. The travel-time residuals of the first *P*-wave (including *P*, P_{diff} and PKP) show systematic spatial variations. The peak-to-peak amplitude in the study area is about 2.0 s. Most part of the Rio Grande Rift has a positive anomaly of about 0.5 s, and the area covered by transitional crust is characterized by overwhelmingly positive residuals of as large as 1.5 s. While the thick sedimentary cover in the extended areas contributes to the observed positive anomalies, calculations using reasonable assumptions of thickness and velocity anomalies of the sedimentary cover suggest that a significant amount of the travel-time delays must come from the mantle, most likely as a result of a thinner lithosphere relative to the continental interior.

Seismic tomography studies suggest that the root of cratons dips toward the interior at greater depth (Burdick et al., 2012; James et al., 2001). Therefore, there is no single definition of the edge that can represents the entire lithosphere. If we use the contour line of 0.25 s (the thick white lines in Fig. 8), which is the average residual in the study area, to approximately represent the edge of the cratonic lithosphere, the eastern boundary of the Rio Grande Rift and the northern boundary of the area with

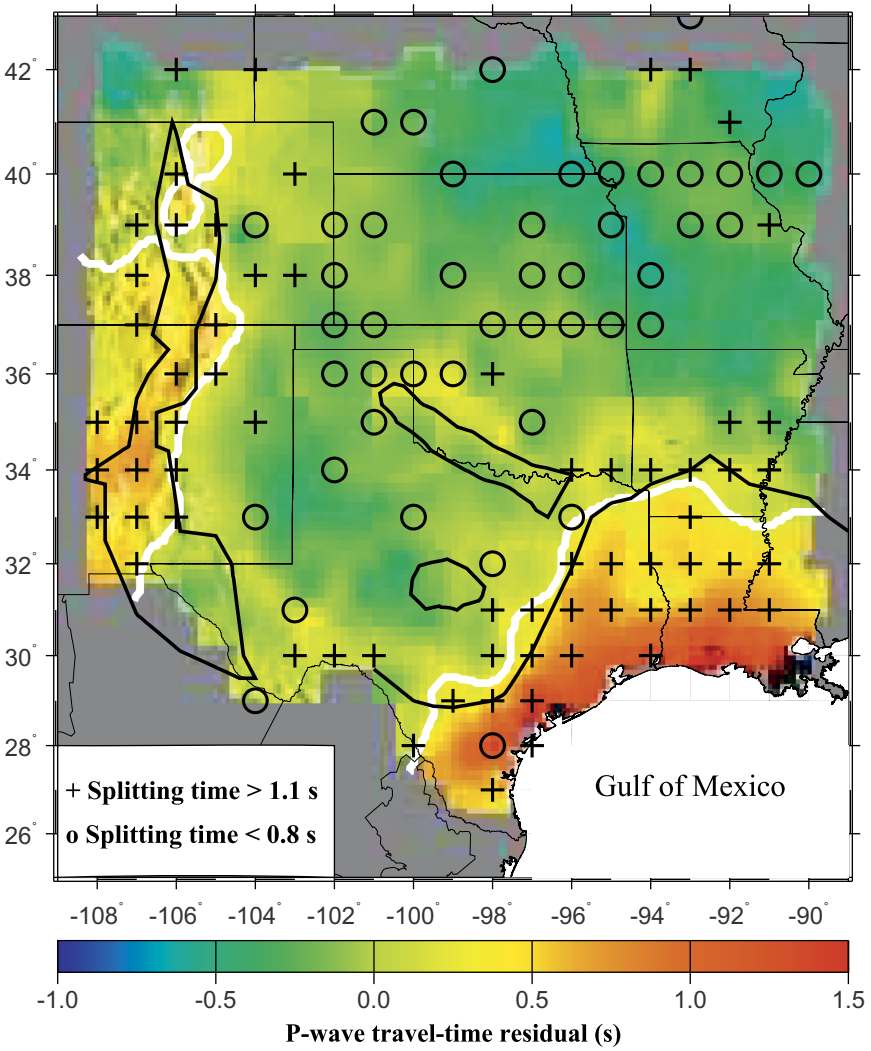

Fig. 8. Spatial correspondence between shear-wave splitting times and teleseismic *P*-wave travel-time residuals. The white lines are smoothed 0.25 s contours. The largest shear-wave splitting times (pluses) are found along the margins of the North American craton, while the smallest values (circles) mostly locate in the interior of the craton. (For interpretation of the references to color in this figure legend, the reader is referred to the web version of this article.)

transitional crust are almost consistent with the cratonic edge (Fig. 8). Note that under this definition, the southwestern corner of the craton extends beyond the US-Mexican border, into an area that has not been sufficiently covered by seismic stations. This is consistent with results from a recent *P*-wave tomography study using USArray data (Burdick et al., 2012).

5.4. Arguments against significant lithospheric contributions to observed anisotropy

In the study area, two anisotropy-forming mechanisms in the lithosphere have been proposed (Barruol et al., 1997; Gao et al., 2008). The first is LPO of olivine *a*-axis under uniaxial compression which leads to a fast direction that is perpendicular to the shortening direction, and the other is the presence of vertical magmatic dikes which result in dike-parallel fast directions. Based on a limited number of SWS measurements, some previous studies (Silver and Chan, 1988; Silver, 1996; Barruol et al., 1997; Gao et al., 2008) proposed a lithospheric origin for the observed anisotropy beneath the North American craton. As argued below, neither mechanism seems to be the dominant cause of the observed *XKS* anisotropy beneath the study area.

Although the parallelism between the APM and most portions of the Proterozoic sutures makes it difficult to distinguish contributions from the lithosphere and asthenosphere, several lines of evidence suggest that collisional orogenies associated with the suture zones did not create significant vertically coherent deformation in the lithosphere, for the following reasons:

(1) The suture zones are not associated with zones of large splitting times. Because the maximum compressional strain is expected to be found along the suture zones, if such strain is responsible for the observed anisotropy, the splitting times in the vicinity of the suture zones should be greater than those in the interior of the Proterozoic provinces. This is not observed for either suture zones (Fig. 5). On the contrary, the smallest splitting times in the entire study area are found in the vicinity of the Yavapai–Mazatzal suture (Fig. 5).
(2) The fast directions do not follow the strike of the suture zones. Most part of the Mazatzal–Grenville suture is not parallel to the APM (Fig. 4). Instead, its strike varies significantly. Such variations are not consistent with the fast directions in the vicinity of the zone, which are dominantly parallel to the APM. Most of the fast directions in the vicinity of the Yavapai–Mazatzal suture zone also show a significant angle with the strike of the zone (Fig. 4).
(3) Both suture zones extend westward to the western US orogenic zone with a NE–SW or NNE-SSW strike, but the fast directions in the orogenic zone and the western margin of the Great Plains are mostly N–S.
(4) The splitting times do not increase with increasing thickness of the lithosphere. Under the assumption of constant lithospheric anisotropy in the study area, areas with thicker lithosphere (i.e., smaller travel-time residuals) should correspond to greater splitting times. Such a positive correlation is not observed. In contrast, the largest observed splitting times are found beneath areas with extended crust on the western and southern margins of the craton, and the smallest splitting times are located in the continental interior where the lithosphere is the thickest (Fig. 8).

Due to chemical or thermal (for recent dikes) contrasts with surrounding rocks, vertical or near-vertical dikes in the lithosphere especially those associated with continental rifting and formation of passive margins can produce mechanical anisotropy. This mechanism was proposed as a possible cause for the observed seismic anisotropy in the Baikal and East African Rift zones (Gao et al., 1997; Kendall et al., 2005) and the north margin of the Gulf of Mexico (Gao et al., 2008). The dikes are expected to be parallel to the rifts or margins. While such dikes can explain the N–S oriented fast directions in the northern half of the Rio Grande Rift, which has a N–S strike, they are unlikely to be responsible for those observed on the southern half of the rift, because the strike of the rift turns southeastward but the fast directions remain N–S (Fig. 4). In addition, N–S fast directions are observed across a wide zone of several hundred kilometers away from the rift axis, and it is unlikely that rift-parallel lithospheric dikes can extend this far from the rift axis (Fig. 4).

The fast directions observed on the transitional crust north of the Gulf of Mexico are parallel to the coastline (Fig. 4), and thus in principle can be attributed to margin-parallel dikes. However, as evidenced by gravity and magnetic data (Mickus et al., 2009), the western margin of the Gulf of Mexico is equally magmatic, and the associated dikes are mostly to be oriented parallel to the coastline, which is N–S. The observed fast directions in this area are mostly NE–SW (Fig. 4) and thus are not consistent with a dike origin.

The above arguments, plus the results of depth estimates using spatial coherency of SWS parameters (Fig. 7), suggest an overall asthenospheric origin for the observed anisotropy. But they do not exclude observable lithospheric contributions for some of the areas. One such area is the Llano Uplift. The top layer could be in the lithosphere and could be formed during the Mesozoic when the Northern American plate was moving toward the north (Yuan and Romanowicz, 2010). Some NW–SE oriented fast directions in the vicinity of the Southern Oklahoma Aulacogen could also reflect fabrics in the lithosphere.

5.5. Asthenospheric origin of anisotropy: a preliminary model

The evidence presented above for the lack of significant lithospheric contribution to the observed anisotropy, especially the results of depth estimate using spatial coherency of splitting parameters (Fig. 7), suggests that most of the observed anisotropy has an origin in the upper asthenosphere. The anisotropic layer corresponding to the observed splitting times has a thickness of about 100 km (assuming a 4% anisotropy), which is inconsistent with the existence of an ultra-thin, low viscosity layer at the base of the lithosphere (Craig and McKenzie, 1986). Such APM-parallel anisotropy in the upper asthenosphere is indicative of a certain degree of lithosphere–asthenosphere coupling (Marone and Romanowicz, 2007). Numerical modeling suggests that large viscosity difference of 8–10 orders of magnitude can lead to decoupling between the lithosphere and asthenosphere (Doglioni et al., 2011). Therefore, the observed anisotropy suggests a viscosity difference that is smaller than 8–10 orders of magnitude.

Beneath the study area and most part of the western US orogenic zone, geodynamic modeling and seismic tomography studies (Becker et al., 2006; Forte et al., 2007) suggest a dominantly northeastward-directed asthenospheric flow (relative to the lithosphere), probably induced by the sinking of the Farallon plate in the lower mantle beneath the New Madrid seismic zone which is located at the eastern edge of our study area. We propose that beneath the western US orogenic zone and the western margin of the Great Plains, the southwestward moving (relative to the asthenosphere) continental root deflects asthenospheric flow along its edge (Fig. 9). The flow moves southward and forms N–S oriented seismic anisotropy (V_A in Fig. 10). This flow system turns eastward around the southwest corner of the root, which is beneath northern Mexico, as suggested by the nearly E–W fast

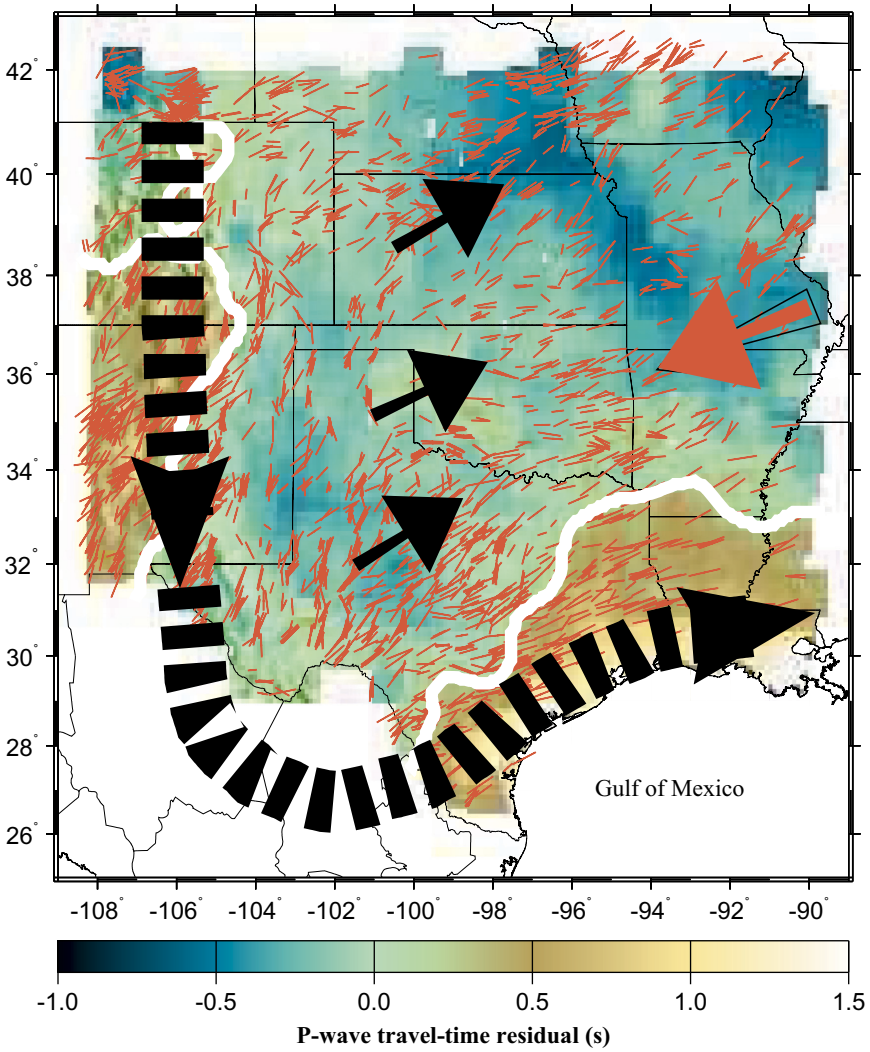

Fig. 9. Schematic diagram showing direction of flow lines in the asthenosphere relative to the lithosphere. The solid black arrows indicate shear-strain in the asthenosphere beneath the craton, and the thick dashed line represents flow deflected by the root of the North American craton. The red arrow shows the APM direction of the North American plate, and the thin red bars represent individual shear-wave splitting measurements (Fig. 4). The background image shows *P*-wave travel-time residuals, and the white lines indicate the approximate edge of the craton (Fig. 8).

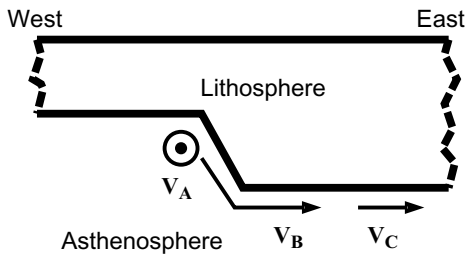

Fig. 10. Conceptual model showing various components of the mantle flow field. The circle with a dot represents southward moving deflected flow around the western cratonic root with velocity V_A, the bended arrow indicates deflected flow beneath the lithosphere with velocity V_B, and the short arrow represents flow in the asthenosphere induced by partial coupling between the lithosphere and asthenosphere with velocity V_C. The sense of motion is relative to the lithosphere.

directions approximately at (103°W, 29.5°N). To a certain extent, the asthenospheric flow system created by the movement of the cratonic root in a low-viscosity asthenosphere is analogous to the so-called escape tectonics observed on the Tibetan Plateau (Zhang et al., 2004). The northward movement of the relatively rigid Indian plate produces eastward flow of the Tibetan lithosphere. At the NE corner of the Indian continent, the flow turns southward, as indicated by surface geology and GPS observations (Zhang et al., 2004).

Depending on the 3-D distribution of viscosity and density in the asthenosphere, it is reasonable to assume that a portion of the flow deflected by the cratonic root of North America goes beneath the root (V_B in Fig. 10). In addition, regardless the existence of the root, the relative movement and partial coupling between the lithosphere and asthenosphere can also lead to simple flow in the upper asthenosphere (V_C in Fig. 10; Conrad and Behan, 2010). Both V_B and V_C contribute to the observed APM-parallel anisotropy. Due to the northward increase of horizontal resistance to southward flow, the magnitude of V_A probably decreases toward the north, as evidenced by the northward decrease in observed splitting times in the area dominated by N–S fast directions. Near the northern extreme of the Rio Grande Rift, the fast directions are spatially varying (Fig. 4), and the splitting times are anomalously small relative to other areas in the western US orogenic zone (Fig. 5). This could suggest that V_A becomes insignificant beneath this area.

The APM-parallel anisotropy beneath the continental interior can be attributed to simple shear strain caused by the relative movement between the base of the lithosphere and a layer with a thickness of about 100 km at the top of the asthenosphere. The

small splitting times observed in the continental interior can be explained by the great depth of the layer, as numerical experiments demonstrate that olivine LPO is better developed at shallower depth in the asthenosphere (Tommasi et al., 2004).

6. Conclusions

Systematic spatial and azimuthal variations of shear-wave splitting parameters are observed beneath the southwestern edge of the North American craton and adjacent areas with unprecedented spatial resolution. Spatial coherency analysis of the splitting parameters suggests that the observed anisotropy is mostly from the upper asthenosphere, implying a certain degree of coupling between the lithosphere and the asthenosphere. The systematic variations and the depth distribution of the source of anisotropy can be adequately interpreted by the southwestward movement of the lithosphere relative to the asthenosphere. The root of the craton orients mantle flow to form strong anisotropy with LPO of olivine *a*-axis parallel to the edge of the craton. In addition, beneath the continental interior, shear-strain in the top layer of the asthenosphere from the relative movement of the lithosphere is the most likely source of APM-parallel anisotropy.

Teleseismic *P*-wave travel time residuals indicate that the southwestern extreme of the North American craton is located in northern Mexico, an area that has not been investigated using broadband seismic data. A seismic experiment with USArray-comparable station density in this area is needed to locate the edge and image the mantle structure. Those results, when combined with results from geodynamic modeling, are essential to test various models regarding continental structure and dynamics, including the mantle flow model presented in this study.

Acknowledgments

Data used in the study were obtained from the IRIS DMC. We thank C. Conrad, A. Eckert, and A. Elsheihk for discussions about mantle flow. Constructive reviews by two anonymous reviewers and Editor P. Shearer significantly improved the manuscript. This study was supported by the US National Science Foundation under Grants EAR-0952064 and EAR-1009946 to K.L. and S.G.

References

Balch, R.S., Hartse, H.E., Sanford, A.R., Lin, K.W., 1997. A new map of the geographic extent of the Socorro mid-crustal magma body. Bull. Seismol. Soc. Am. 87, 174–182.

Baldridge, W.S., Perry, F.V., Vaniman, D.T., Nealey, L.D., Leavy, B.D., Laughlin, A.W., Kyle, P.R., Bartov, Y., Steintz, G., Gladney, E.S., 1991. Middle to late Cenozoic magmatism of the southeastern Colorado Plateau and central Rio Grande rift (New Mexico and Arizona, USA: a model for continental rifting. Tectonophysics 197, 327–354.

Barruol, G., Hoffmann, R., 1999. Upper mantle anisotropy beneath the Geoscope stations. J. Geophys. Res. 104, 10757–10773.

Barruol, G., Silver, P.G., Vauchez, A., 1997. Seismic anisotropy in the eastern United States: deep structure of complex continental plate. J. Geophys. Res. 102, 8329–8348, http://dx.doi.org/10.1029/96JB03800.

Becker, T.W., O'Connell, R., 2001. Predicting plate velocities with mantle circulation models. Geochem. Geophys. Geosyst. 2, http://dx.doi.org/10.1029/2001GC000171.

Becker, T.W., Schulte-Pelkum, V., Blackman, D.K., Kellogg, J.B., O'Connell, R.J., 2006. Mantle flow under the western United States from shear wave splitting. Earth Planet. Sci. Lett. 247, 1501–1507.

Bird, P., Liu, Z., Rucker, W.K., 2008. Stress that drive the plates from below: definitions, computational path, model optimization, and error analysis. J. Geophys. Res. 113, B11406, http://dx.doi.org/10.1029/2007JB005460.

Burdick, S., Van Der Hilst, R.D., Vernon, F.L., Martynov, V., Cox, T., Eakins, J., Karasu, G.H., Tylell, J., Astiz, L., Pavlis, G.L., 2012. Model update March 2011: upper mantle heterogeneity beneath North America from traveltime tomography with global and USArray Transportable Array data. Seismol. Res. Lett. 83, 23–28, http://dx.doi.org/10.1785/gssrl.83.1.23.

Condie, K.C., 1982. Plate-tectonics model for Proterozoic continental accretion in the southwestern United States. Geology 10, 37–42.

Conrad, C.P., Behan, M.D., Silver, P.G., 2007. Global mantle flow and the development of seismic anisotropy: differences between the oceanic and the continental upper mantle. J. Geophys. Res. 112, B07317, http://dx.doi.org/10.1029/2006JB004608.

Conrad, C.P., Behan, M.D., 2010. Constraints on lithosphere net rotation and asthenospheric viscosity from global mantle flow models and seismic anisotropy. Geochem. Geophys. Geosyst. 11, Q05W05, http://dx.doi.org/10.1029/2009GC002970.

Coward, M.P., Butler, R.W.H., Khan, M.A., Knipe, R.J., 1987. The tectonic history of Kohistan and its implications for Himalayan structure. J. Geol. Soc., London 144, 377–391.

Craig, C.H., McKenzie, D., 1986. The existence of a thin low-viscosity layer beneath the lithosphere. Earth Planet. Sci. Lett. 78, 420–426.

Debayle, E., Kennett, B.L.N., Priestley, K., 2005. Global azimuthal seismic anisotropy and the unique plate-motion deformation of Australia. Science 433, 509–512.

Doglioni, C., Ismail-Zadeh, A., Panza, G., Riguzzi, F., 2011. Lithosphere–asthenosphere viscosity contrast and decoupling. Phys. Earth Planet. Inter. 189, 1–8.

Evans, M.S., Kendall, J.-M., Willemann, R.J., 2006. Automated SKS splitting and upper-mantle anisotropy beneath Canadian seismic stations. Geophys. J. Int. 165, 931–942, http://dx.doi.org/10.1111/j.1365-246X.2006.02973.x.

Forte, A.M., Mitrovica, J.X., Moucha, R., Simmons, N.A., Grand, S.P., 2007. Descent of the ancient Farallon slab drives localized mantle flow below the New Madrid seismic zone. Geophys. Res. Lett. 34, L04308, http://dx.doi.org/10.1029/2006GL027895.

Fouch, M.J., Fischer, K.M., Parmentier, E.M., Wysession, M.E., Clarke, T.J., 2000. Shear wave splitting, continental keels, and pattern of mantle flow. J. Geophys. Res. 105, 6255–6275.

Fouch, M.J., Rondenay, S., 2006. Seismic anisotropy beneath stable continental interiors. Phys. Earth Planet. Inter. 158, 292–320, http://dx.doi.org/10.1016/j.pepi.2006.01.022.

Gao, S.S., Davis, P.M., Liu, K.H., Slack, P.D., Rigor, A.W., Zorin, Y.A., Mordvinova, V.V., Kozhevnikov, V.M., Logatchev, N.A., 1997. *SKS* splitting beneath continental rift zones. J. Geophys. Res. 102, 22781–22797.

Gao, S.S., Liu, K.H., 2009. Significant seismic anisotropy beneath the southern Lhasa Terrane, Tibetan Plateau. Geochem. Geophys. Geosyst. 10, Q02008 http://dx.doi.org/10.1029/2008GC002227.

Gao, S.S., Liu, K.H., 2012. AnisDep: a FORTRAN program for the estimation of the depth of anisotropy using spatial coherency of shear-wave splitting parameters. Comput. Geosci. http://dx.doi.org/10.1016/j.cageo.2012.01.020.

Gao, S.S., Liu, K.H., Abdelsalam, M.G., 2010. Seismic anisotropy beneath the Afar Depression and adjacent areas: implications for mantle flow. J. Geophys. Res. 115, B12330, http://dx.doi.org/10.1029/2009JB007141.

Gao, S.S., Liu, K.H., Stern, R.J., Keller, G.R., Hogan, J.P., Pulliam, J., Anthony, E.Y., 2008. Characteristics of mantle fabrics beneath the south-central United States: Constraints from shear-wave splitting measurements. Geosphere 4, 411–417, http://dx.doi.org/10.1130/GES00159.1.

Gok, R., Ni, J., Sandvol, E., Wilson, D., Baldridge, W.S., Aster, R., West, M., Grand, S., Gao, W., Tilmann, F., Semken, S., 2003. Shear wave splitting and mantle flow beneath the LA RISTRA array. J. Geophys. Res. 115, B12330http://dx.doi.org/10.1029/2009JB007141.

Gripp, A.E., Gordon, R.G., 2002. Young tracks of hotspots and current plate velocities. Geophys. J. Int. 150, 321–361.

Hoffman, P.F., 1988. United plates of America, the birth of a craton: early Proterozoic assembly and growth in Laurentia. Annu. Rev. Earth Planet. Sci. 16, 543–603.

Hoffman, P.F., 1989. Precambrian geology and tectonic history of North America. In: Bally, A.W., Palmer, A.R. (Eds.), The geology of North America—An overview. Geological Society of America, pp. 447–512.

Holtzman, B.K., Kohlstedt, D.L., Zimmerman, M.E., Heidelbach, F., Hiraga, T., Hustoft, J., 2003. Melt segregation and strain partitioning: implications for seismic anisotropy and mantle flow. Science 301, 1227–1230 . 10.1126/science.1087132.

Holm, D.K, Anderson, R., Boerboom, T.J., Cannon, W.F., Chandler, V., Jirsa, M., Miller, J., Schneider, D.A., Schulz, K.J., Van Schmus, W.R., 2007. Reinterpretation of Paleoproterozoic accretionary boundaries of the north-central United States based on a new aeromagnetic-geologic compilation. Precambrian Research 157, 71–79.

Huang, Z., Wang, L., Zhao, D., Mi, N., Xu, M., 2011. Seismic anisotropy and mantle dynamics beneath China. Earth Planet. Sci. Lett. 306, 105–117.

James, D.E., Fouch, M.J., Vandecar, J.C., van der Lee, S., 2001. Kaapvaal Seismic Group, 2001. Tectospheric structure beneath southern Africa. Geophys. Res. Lett. 28, 2485–2488.

Karato, S., Jung, H., Katayama, I., Skemer, P., 2008. Geodynamic significance of the seismic anisotropy of the upper mantle: new insights from laboratory studies. Annu. Rev. Earth Planet. Sci. 36, 59–95.

Karlstrom, K.E., Bowring, S.A., 1988. Early Proterozoic assembly of tectono-stratigraphic terranes in southwestern North America. J. Geol. 96, 561–576.

Kendall, J.-M., Stuart, G.W., Ebinger, C., Bastow, I.D., Keir, D., 2005. Magma-assisted rifting in Ethiopia. Nature 433, 146–148.

Kennett, B.L.N., Engdahl, E.R., 1991. Traveltimes for global earthquake location and phase identification. Geophys. J. Int. 105, 429–465.

Lawton, T.F., McMillan, N.J., 1999. Arc abandonment as a cause for passive continental rifting: comparison of the Jurassic Mexican Borderland rift and the Cenozoic Rio Grande rift. Geology 27, 779–782.

Liu, K.H., 2009. NA-SWS-1.1: a uniform database of teleseismic shear-wave splitting measurements for North America. Geochem. Geophys. Geosyst. 10, Q05011, http://dx.doi.org/10.1029/2009GC002440.

Liu, K.H., Gao, S.S., 2010. Spatial variations of crustal characteristics beneath the Hoggar swell, Algeria revealed by systematic analyses of receiver functions from a single seismic station. Geochem. Geophys. Geosys. 11, Q08011, http://dx.doi.org/10.1029/2010GC003091.
Liu, K.H., Gao, S.S., 2011. Estimation of the depth of anisotropy using spatial coherency of shear-wave splitting parameters. Bull. Seismol. Soc. Am. 101, 2153–2161.
Liu, K.H., Gao, S.S., Gao, Y., Wu, J., 2008. Shear wave splitting and mantle flow associated with the deflected slab beneath northeast Asia. J. Geophys. Res. 113, B01305, http://dx.doi.org/10.1029/2007JB005178.
Liu, L., Gurnis, M., 2010. Dynamic subsidence and uplift of the Colorado Plateau. Geology 38, 719–722.
Long, M.D., Silver, P.G., 2009. Shear wave splitting anisotropy: measurements, interpretation, and new directions. Surv. Geophys. 5, 407–461.
Mainprice, D., Barruol, G., Ben Ismail, W., 2000. The seismic anisotropy of the Earth's Mantle: from single crystal to polycrystal. In: Karato, S.I. (Ed.), Earth's Deep Interior. AGU, Washington, DC, pp. 237–264.
Marone, F., Romanowicz, B., 2007. The depth distribution of azimuthal anisotropy in the continental upper mantle. Nature 447, 198–201.
McMillan, J., Dickin, A.P., Haag, D., 2000. Evolution of magma source regions in the Rio Grande rift, southern New Mexico. Geol. Soc. Am. Bull. 112, 1582–1593.
Mickus, K., Stern, R.J., Keller, G.R., Anthony, E.Y., 2009. Potential field evidence for a volcanic rifted margin along the Texas Gulf Coast. Geology 37, 387–390, http://dx.doi.org/10.1130/G25465A.1.
Montagner, J., 1998. Where can seismic anisotropy be detected in the Earth's mantle? In boundary layers …. Pure Appl. Geophys. 151, 223–256.
Morgan, P., Seager, W.R., Golombek, M.P., 1986. Cenozoic thermal mechanical and tectonic evolution of the Rio Grande rift. J. Geophys. Res. 91, 6262–6276.
Mosher, S., 1998. Tectonic evolution of the southern Laurentian Grenville orogenies belt. Geol. Soc. Am. Bull. 110, 1357–1375.
Nicolas, A., 1993. Why fast polarization directions of SKS seismic waves are parallel to mountain belts. Phys. Earth Planet. Inter. 78, 337–342.
Nicolas, A., Christensen, N.I., 1987. Formation of anisotropy in upper mantle peridotites: a review. In: Fuchs K., Froidevaux, C. (Eds.), Composition Structure and Dynamics of the Lithosphere–Asthenosphere System. Geodynamics Series, vol. 16, pp. 338–343.
Sandvol, E., Ni, J., Ozalaybey, S., Schlue, J., 1992. Shear-wave splitting in the Rio Grande Rift. Geophys. Res. Lett. 19, 2337–2340, http://dx.doi.org/10.1029/92GL02715.
Sandvol, E., Ni, J., 1994. Mapping seismic azimuthal anisotropy in the United States from LRSM short period data. Eos, Trans. AGU 75, 481.
Savage, M.K., 1999. Seismic anisotropy and mantle deformation: what we learned from shear-wave splitting?. Rev. Geophys. 37, 65–106.
Savage, M.K., Sheehan, A.F., 2000. Seismic anisotropy and mantle flow from the Great Basin to the Great Plains, western United States. J. Geophys. Res. 151, 443–462.
Savage, M.K., Sheehan, A.F., Lerner-Lam, A., 1996. Shear wave splitting across the Rocky Mountain Front. Geophys. Res. Lett. 23, 2267–2270.
Silver, P.G., 1996. Seismic anisotropy beneath the continents: probing the depths of geology. Annu. Rev. Earth Planet. Sci. 24, 385–432.
Silver, P.G., Chan, W.W., 1988. Implications for continental structure and evolution from seismic anisotropy. Nature 335, 34–39.
Silver, P.G., Chan, W.W., 1991. Shear wave splitting and subcontinental mantle deformation. J. Geophys. Res. 96, 16429–16454.
Silver, P.G., Savage, M., 1994. The interpretation of shear-wave splitting parameters in the presence of two anisotropic layers. Geophys. J. Int. 119, 949–963, http://dx.doi.org/10.1111/j.1365-246X.1994.tb04027.x.
Thomas, W.A., 2006. Tectonic inheritance at a continental margin. GSA Today 16, 4–11.
Tommasi, A., Mainprice, D., Cordier, P., Thoraval, C., Couvy, H., 2004. Strain-induced seismic anisotropy of wadsleyite polycrystals and flow patterns in the mantle transition zone. J. Geophys. Res. 109, B12405, http://dx.doi.org/10.1029/2004JB003158.
Vandecar, J.C., Crossen, R.S., 1990. Determination of teleseismic relative phases arrival times using multi-channel cross-correlation and least-squares. Bull. Seismol. Soc. Am. 80, 150–169.
van der Lee, S., Frederiksen, A., 2005. Surface wave tomography applied to the North American upper mantle. In: Nolet, G., Levander, A. (Eds.), Seismic Data Analysis and Imaging with Global and Local Arrays. American Geophysical Union Monograph, vol. 157, pp. 67–80.
van der Lee, S., Nolet, G., 1997. Upper mantle S velocity structure of North America. J. Geophys. Res. 102, 22,815–22,838, http://dx.doi.org/10.1029/97JB01168.
Vinnik, L.P., Makeyeva, L.J., Milev, A., Usenko, A.Y., 1992. Global patterns of azimuthal anisotropy and deformations in the continental mantle. Geophys. J. Int. 111, 433–447.
Waite, G.P., Schutt, D.L., Smith, R.B., 2005. Models of lithosphere and asthenosphere anisotropic structure of the Yellowstone hot spot from shear wave splitting. J. Geophys. Res. 110, http://dx.doi.org/10.1029/2004JB003501.
Walker, K.T., Nyblade, A.A., Klemperer, S.L., Bokelmann, G., Owens, T.J., 2004. On the relationship between extension and anisotropy: constraints from shear wave splitting across the East African Plateau. J. Geophys. Res. 109, B08302, http://dx.doi.org/10.1029/2003JB002866.
Wang, X., Ni, J.F., Aster, R., Sandvol, E., Wilson, D., Sine, C., Grand, S.P., Baldridge, W.S., 2008. Shear-wave splitting and mantle flow beneath the Colorado Plateau and its boundary with the Great Basin. Bull. Seismol. Soc. Am. 98, 2526–2532.
Whitmeyer, S.J., Karlstrom, K.E., 2007. Tectonic model for the Proterozoic growth of North America. Geosphere 34, 220–259.
Wilson, D., Aster, R., West, W., Ni, J., Grand, S., Gao, W., Baldridge, W.S., Patel, P., 2005. Lithospheric structure of the Rio Grande rift. Nature 433, 851–855.
Yuan, H., Romanowicz, B., 2010. Lithospheric layering in the North American craton. Nature 466, 1063–1069.
Zhang, P.-Z., Shen, Z.K., et al., 2004. Continuous deformation of the Tibetan Plateau from global positioning system data. Geology 32, 809–812, http://dx.doi.org/10.1130/G20554.1.
Zhang, S., Karato, S.I., 1995. Lattice preferred orientation of olivine aggregates deformed in simple shear. Nature 375, 774–777.